Solar Energy xxx (xxxx) xxx–xxx

Contents lists available at ScienceDirect

Solar Energy

journal homepage: www.elsevier.com/locate/solener

# High-field magnetotransport in $Cu_2ZnGeS_4$ single crystals

Elena Hajdeu-Chicarosh[a,b,*], Erkki Lähderanta[a], Maxim Guc[a,b], Konstantin Lisunov[a,b], Mikhail Shakhov[a,c], Ivan Zakharchuk[a], Serghei Levcenko[d], Ernest Arushanov[b]

[a] Department of Mathematics and Physics, Lappeenranta University of Technology, PO Box 20, FIN-53851 Lappeenranta, Finland
[b] Institute of Applied Physics, Academy of Sciences of Moldova, Academiei Str. 5, MD-2028 Chisinau, Republic of Moldova
[c] Ioffe Institute, Politehnicheskaya Str. 26, St. Petersburg 194021, Russian Federation
[d] Helmholtz Zentrum Berlin für Materialien und Energie, Hahn-Meitner-Platz 1, D-14109 Berlin, Germany

ARTICLE INFO

*Keywords:*
Quaternary chalcogenides
Hopping conduction
Magnetoresistance
Hall effect

ABSTRACT

The quaternary chalcogenides, attracting much attention in recent time as promising solar energy materials, permit an effective optimization of their composition by the Ge incorporation. In particular, this implies an interest to the $Cu_2ZnGeS_4$ compound, which utilization requires, however, a deeper understanding of its electronic properties in general. Here, we investigate magnetotransport of the *p*-type $Cu_2ZnGeS_4$ single crystals, including resistivity, ρ (*T*), magnetoresistance (MR) and Hall effect, in pulsed magnetic fields up to $B = 20$ T. The Mott variable-range hopping charge transfer has been established within a broad temperature interval of *T* between ~100 and 200 K by investigations of ρ (*T*) in zero field. The positive and negative contributions to MR have been observed, attributing them to shrinkage of the impurity wave functions by the magnetic field and to the destructive interference of the hopping charge carriers, respectively. Observation of the *negative* Hall coefficient, $R_H$ (*T*), exhibiting the dependence close to that of ρ (*T*), gives a strong support to the Mott conduction mechanism in our *p*-type $Cu_2ZnGeS_4$ material. In addition, the conductivity, connected with thermal activation of holes on the mobility edge, $E_c$, has been identified both below and above the Mott conduction interval. Finally, the joint analysis of the ρ (*T*) and MR data has yielded a series of important microscopic parameters. These include such details of the hole spectrum in the acceptor band, as its semi-width, *W*, the density of localized states, *g* (μ), at the Fermi level, μ, the positions of μ and $E_c$, as well as values of the localization radius of holes, *a*, and of the acceptor concentration, $N_A$.

## 1. Introduction

Interest to the quaternary group $I_2$-II-IV-$VI_4$ chalcogenide semiconductors is connected mainly with their attractive photovoltaic properties, permitting effective utilization of the compounds as solar energy materials (Siebentritt and Schorr, 2012; Polizzotti et al., 2013; Adachi, 2015). Indeed, an efficiency up to 12.6% has been achieved recently in $Cu_2ZnSn(S,Se)_4$ based solar cells (Wang et al., 2014), whereas optimization of the material composition by a partial cation substitution is expected to provide its further increase. In this way, incorporation of Ge is quite promising as has been shown recently by investigations of the $Cu_2ZnSn_xGe_{1-x}(S,Se)_4$ solid solutions (Guo et al., 2012; Kim et al., 2014; Hages et al., 2015), whereas even a small doping of the $Cu_2ZnSnSe_4$ layers with Ge has resulted in a real increase of the solar cell efficiency (Giraldo et al., 2015, 2016). Another possibility of development of the solar energy science and technology is connected to designing new devices with materials of interest. In particular, much attention has been paid recently to tandem solar cells with a quaternary compound utilized as a top element with an increased band gap, $E_g$ (White et al., 2014; Umehara et al., 2016; Todorov et al., 2014). In this context, the $Cu_2ZnGeS_4$ (CZGeS) compound, belonging to the quaternary chalcogenide semiconductor family above, and having $E_g \sim 2$ eV (León et al., 2010; Levcenco et al., 2011) and the absorption coefficient above $10^4$ $cm^{-1}$ (León et al., 2010), is quite available for such utilization. Beyond the photovoltaics, CZGeS has demonstrated attractive features as an effective agent for the hydrogen evolution of water (Tsuji et al., 2010), as well as a prospective material for thermoelectric devices (Heinrich et al., 2014). Hence, CZGeS exhibits a broad area of possible applications, which, however, requires a deeper knowledge of its fundamental properties.

At this point, extensive structural investigations of CZGeS have revealed two different types, namely the kesterite (Parasyuk et al., 2005; Khadka and Kim, 2013; Valakh et al., 2016; Guc et al., 2016) and wurtzstannite (Yao et al., 1987; Matsushita et al., 2005; Levcenco et al.,

* Corresponding author at: Institute of Applied Physics, Academy of Sciences of Moldova, Academiei Str. 5, MD-2028 Chisinau, Republic of Moldova.
*E-mail address:* elenahajdeu@yahoo.com (E. Hajdeu-Chicarosh).

https://doi.org/10.1016/j.solener.2018.04.043
Received 11 November 2017; Received in revised form 17 April 2018; Accepted 20 April 2018

2011; Schafer and Nitsche, 1974; Guc et al., 2014a) structures. The optical (León et al., 2010; Yao et al., 1987; Matsushita et al., 2005; Levcenco et al., 2011; Guc et al., 2014a; Schleich and Wold, 1977) and vibrational (Guc et al., 2014a, 2016; Garcia-Llamas et al., 2016, 2017; Valakh et al., 2016) properties of both CZTS structural types have been deeply studied, as well. However, a much lesser attention still has been paid to the electronic transport, despite of its high importance in any of the CZGeS utilizations above. In this sense, only a few works could be mentioned, including the room temperature resistivity measurements (Yao et al., 1987; Levcenco et al., 2011; Schleich and Wold, 1977) and their extension to the high-temperature interval (Heinrich et al., 2014; Zeier et al., 2014), requiring however a deeper analysis of the experimental data. More explicit investigations of the magnetotransport have been performed in the $Cu_2ZnSn_xGe_{1-x}Se_4$ solid solutions, exhibiting interesting results but only with the kesterite type samples involved (Lähderanta et al., 2016a).

In the present work, electronic properties of CZGeS single crystals with wurtzstannite structure are studied by a high-field magnetotransport method. This includes measurements of magnetoresistance (MR) and Hall effect, as well as resistivity ρ (*T*) in zero magnetic field, and their subsequent explicit quantitative analysis. The latter, being applied to the results of joint investigations of the MR and ρ (*T*) data, permits determination of fundamental electronic parameters in semiconductors in general (Ionov et al., 1983; Lisunov et al., 1996, 2000; Essaleh and Wasim, 2007), as well as specification of conduction mechanisms within different temperature intervals in quaternary materials of the family above, such as $Cu_2ZnSn_xGe_{1-x}Se_4$ (Lähderanta et al., 2016a) and $Cu_2ZnSnSe_4$ (Lähderanta et al., 2016b) kesterites. In addition, utilization of the CZGeS single crystals suggests a minimum of various extrinsic effects, observed much wider e.g. in polycrystalline thin films and powder materials. This provides a confidence for determination of mostly intrinsic properties of CZGeS, permitting probably their better utilization as important reference data.

## 2. Experimental study

CZGeS single crystals were obtained with chemical vapor transport method, using iodine as a transport agent. All details of the growing process can be found in Levcenco et al. (2011). To account for a possible influence of unavoidable fluctuations during the preparation process, three different CZGeS samples, marked below as S1, S2 and S3, respectively, were chosen (without any specially controlled parameter) for the magnetotransport investigations. In addition, they were selected to have a most convenient shape for electrical measurements. The chemical composition of the material was obtained with the X-ray fluorescent method, and the results from three different sample points were averaged. The data did not exhibit a significant variation from point to point, giving evidence for a close proximity of the composition to stoichiometry for all samples. A part of the investigated material was subjected to the X-ray diffraction analysis, evidencing for the wurtzstannite structure of all the investigated samples.

The *p*-type conductivity of the samples was established with the hot point probe method, performed by the thermopower measurements. Each investigated sample was supplied with six indium contacts. A standard dc method was applied for the measurements of ρ (*T*), whereas MR was studied in a pulsed magnetic field with *B* up to 20 T. The device details can be found in Lähderanta et al. (2016b). The sample was installed on the holder and inserted inside a filling helium cryostat, which was used to vary the sample temperature between 20 and 300 K. A cryostat finger, containing the sample, was inserted inside a pulsed solenoid. The principal sample plate was oriented perpendicular to the magnetic field direction. Any measurement at a certain temperature was made by increasing and decreasing field from 0 up to the values within an interval of *B* ~0.5–20 T, and repeated by changing of the field polarity. A special software was used to average the data with the opposite polarities, yielding the longitudinal (ρ) and the transversal ($\rho_H$) resistivity components and avoiding their mutual influences. To obtain the dependence of ρ (*B*) and $\rho_H$ (*B*) over the whole field diapason, the series of such measurements was integrated. It should be also mentioned existence of certain limitations for the obtained results from the low-temperature side due to a high sample resistivity, exceeding somewhat the device abilities.

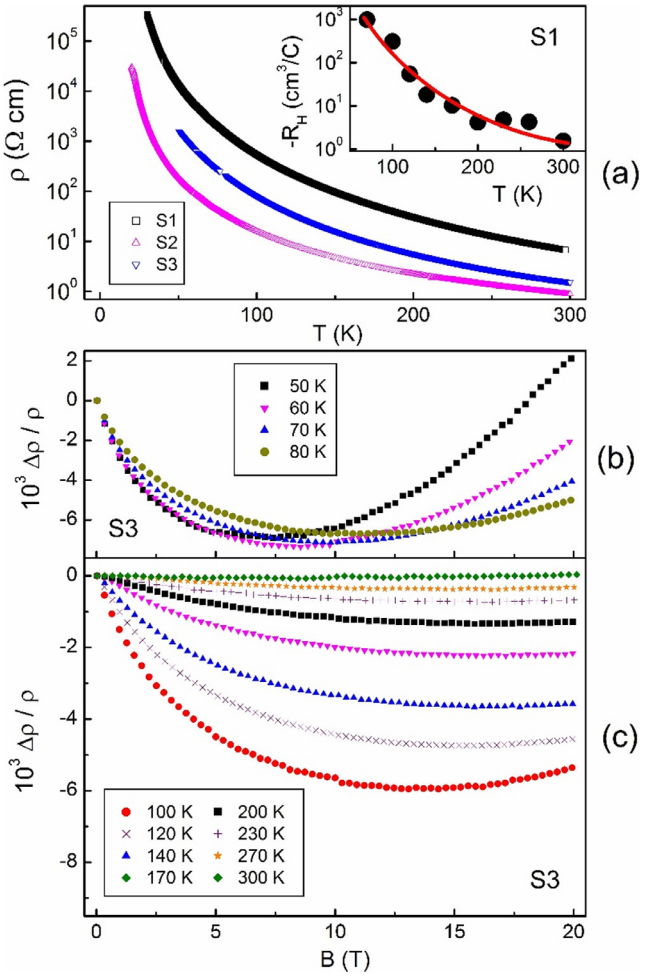


**Fig. 1.** Temperature dependence of resistivity in samples S1, S2 and S3. Inset: The plot of – $R_H$ vs. *T*. The line is a guide to the eye (a). The dependence of MR on the magnetic field for sample S3 at 50–80 K (b) and 100–300 K (c).

## 3. Results and discussion

Temperature dependence of the resistivity is similar for all samples, indicating a strongly activated behavior as evident in Fig. 1(a). The dependences of the relative MR, $\Delta\rho/\rho \equiv [\rho(B) - \rho(0)]/\rho(0)$, are basically similar, too, where an example for sample S3 is displayed in Fig. 1(b) and (c). MR curves contain both the positive (pMR) and the negative (nMR) contributions, whereas the overall MR effect is generally negative almost within the whole temperature range between ~50 and 300 K. In addition, one can see different temperature dependence of MR within two different *T* intervals of 50–80 K and 100–300 K, as presented in Fig. 1(b) and (c), respectively. Namely, a homogeneous decrease of MR, typical of doped semiconductors, takes place only above 80 K, whereas below this temperature the behavior of MR with *T* is more complicated, depending on *B*. The functions of $\rho_H$ (*B*) are close to linear, giving no evidence for a dependence of the Hall coefficient, $R_H$, of *B*. On the other hand, the dependence of $R_H$ (*T*) in the inset to Fig. 1(a) is quite strong and similar to that of ρ (*T*) in Fig. 1(a). In addition, the sign of $R_H$ is negative, despite of the *p*-type conduction